ORIGINAL PAPER

# Seasonal characteristics of the large-scale moisture flux transport over the Arabian Peninsula

H. Athar[1] · K. Ammar[2]

**Abstract** The relationship between the lower tropospheric (1000 to 850 hPa) large-scale moisture flux transport and the precipitation over the Arabian Peninsula (AP), on a seasonal basis, using the NCEP–NCAR gridded dataset for the 53-year period (1958–2010), is investigated. The lower tropospheric moisture flux divergence occurs due to the Hadley cell-based descending air over the AP, as well as due to the presence of Somali jet in dry season (June to September) for the southern ($\leq 22°$ N) AP domain, leading to significantly reduced precipitation in the AP. The AP thus acts more as a net transporter of moisture flux from adjacent Sea areas to nearby regions. The North Atlantic Oscillation (NAO) and the Artic Oscillation (AO) climatic indices are found to modulate significantly the net seasonal moisture flux into the AP region animating from the Mediterranean Sea, and the Arabian Sea, both for the northern ($\geq 22°$ N) and southern AP domains.

## 1 Introduction

The large-scale (in contrast to the meso-scale) moisture flux transport studies are of great contemporary need for arid regions such as the Arabian Peninsula (AP), where water resources management is a priority decision-making aspect for the policy makers (Gimeno et al. 2011, and references cited therein; IPCC 2013). Such studies also provide an analyzed perspective for global climate model projection studies (see, for instance, Jin et al. 2011; Prasanna and Yasunari 2011). Another rewarding aspect of such studies is the contribution toward a better understanding of the role of large-scale moisture flux toward individual precipitation events in the neighboring countries of the AP such as the western Iran (Farajzadeh et al. 2007).

The large-scale moisture flux transport may be described in terms of the specific humidity ($q$) and the wind vector components (Peixoto and Oort 1983). Both of these climatic variables are interactive and play a crucial role in determining other climatic variables such as the various forms of the atmospheric energy, in particular, the latent heat transport from the tropics to the mid-latitudes (Peixoto and Oort 1992; for a recent review of these topics, see, for instance, Sherwood et al. 2010; Trenberth 2011).

The study area including the topographic details is displayed in Fig. 1. The study area is AP, which is situated between the western Asia and the African continent. Areawise, Saudi Arabia is the largest country in the AP, covering almost 80 % of the AP area (Vincent 2008). Saudi Arabia also harbors the world largest continuous sand desert (Edgell 2006). The study area is divided into the southern (12–22° N, 35–60° E) and the northern (22–32° N, 35–60° E) domains in order to study the relationship between the large-scale seasonal moisture flux transport and the precipitation occurrence in the AP and to perform the moisture budget analysis. This division is based on the climatological behavior of precipitation in the AP (see, for instance, Almazroui et al. 2013). The four main water bodies adjacent to the AP include the Mediterranean Sea in the northwest, the Arabian Gulf in the east, the Arabian Sea in the south, and the Red Sea in the west. The northern AP domain includes parts of Saudi Arabia, United Arab Emirates, Oman, Iran, Iraq, Jordan, Egypt, as well as Kuwait, Bahrain, and Qatar (not displayed). The

✉ H. Athar
athar.hussain@comsats.edu.pk

[1] Department of Meteorology, COMSATS Institute of Information Technology, Park Road, Chak Shahzad, Islamabad 44000, Pakistan

[2] Center of Excellence for Climate Change Research, Department of Meteorology, King Abdulaziz University, P. O. Box 80208, Jeddah 21589, Saudi Arabia
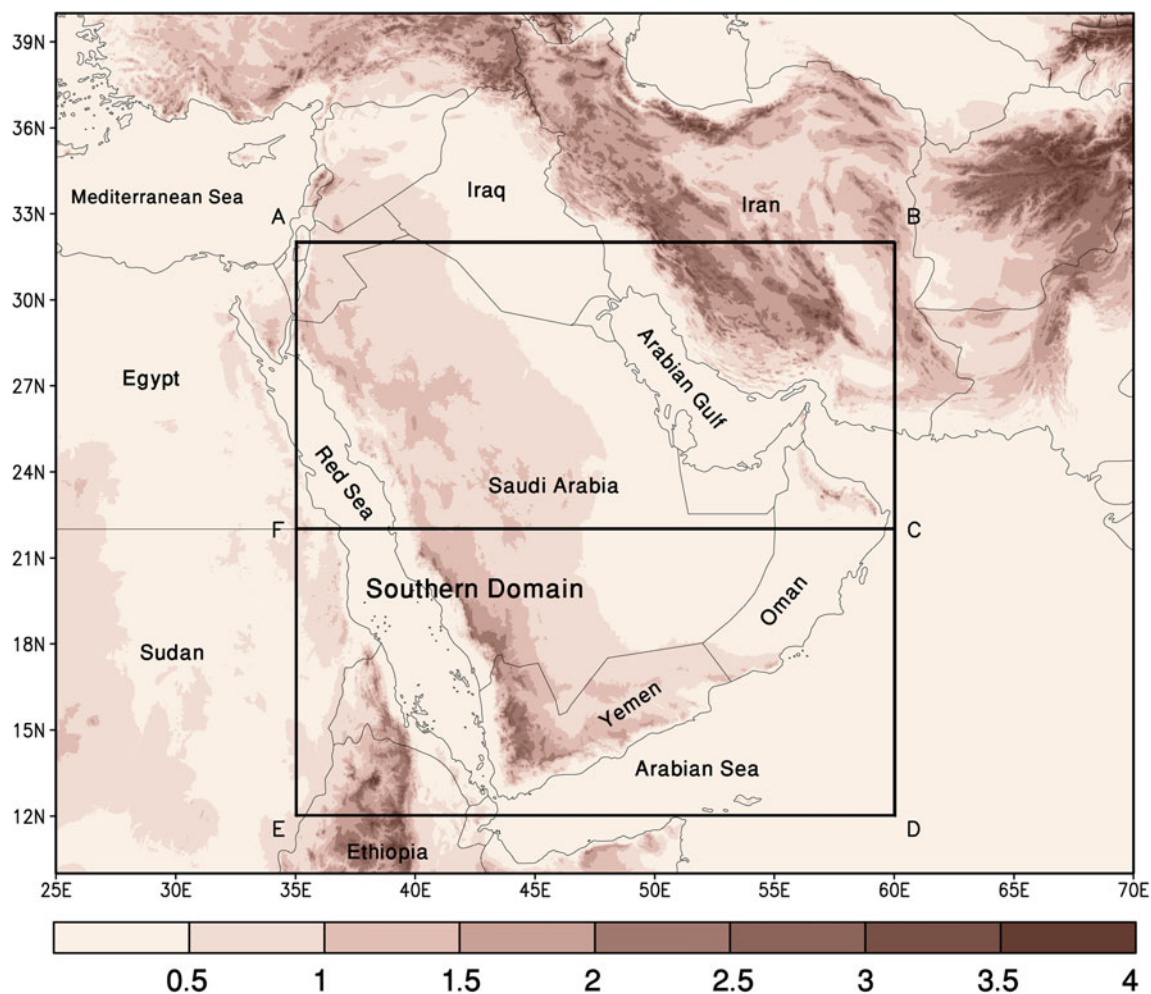
**Fig. 1** The geographical map of the study region. Areas adjacent to the AP, including the Mediterranean Sea, the Red Sea, the Arabian Sea, and the Arabian Gulf, are marked, along with the topography (in kilometers). The displayed southern (12–22° N, 35–60° E) and northern domains (22–32° N, 35–60° E) are used in the moisture budget analysis

southern AP domain includes parts of Saudi Arabia, Sudan, Ethiopia, entire Eritrea (not displayed), entire Oman, and entire Yemen.

Because of the close proximity and intimate relationship of the Findlater/Somali Jet with the Indian/Asian summer monsoon, the study of the Arabian Sea wind and moisture circulations has been the subject of several studies, based on the various climatic datasets (see, for instance, Min and Schubert 1997; Chakraborty et al. 2006a; JianQi et al. 2008, including the pioneering moisture flux analysis over deserts by Starr and Peixoto (1958)). For a description of the surface winds behavior during the active Somali Jet period (May–June), see, for instance, Halpern and Woiceshyn (1999). From the lower to the higher tropospheric pressure values, a shift in the Somali Jet direction toward the south occurs. These attributes of the wind circulations based on the horizontal wind distributions have direct implication for the large-scale moisture flux transport, the consequent large-scale moisture budget as well as for the precipitation patterns in the active Somali Jet period in the AP. Low-dimensional model-based numerical experiments are also performed to study the precipitation dynamics of the Arabian deserts (see, for instance, Charney 1975; Rodwell and Hoskins 1996).

In the AP, climatologically, the precipitation occurrence patterns may be described as follows: During November to April, the precipitation occurs dominantly in the northern AP domain (≥22° N); this period will be referred to as the wet season (Almazroui et al. 2012a). During June to September, the precipitation occurs mostly in the southern AP domain (≤22° N); this period will be referred to as the dry season. The months of May and October are considered as transitional. Generally, the precipitation tends to occur in the form of sporadic and high intensity individual events (see, for instance, Almazroui et al. 2012b). In both the seasons, in the extreme southwestern part of the AP, the precipitation occurs. These temporal and spatial divisions are also used in studying several other aspects of weather and climate of the AP (see, for instance, Athar et al. 2013; Athar 2014, 2015). We henceforth consider these spatial and temporal divisions to study the

seasonal characteristics of the large-scale moisture flux and its associated large-scale moisture flux budget.

No updated view of the large-scale moisture flux transport over the AP is available (to our knowledge) though individual precipitation case studies in the AP are available. Depending upon the location of the precipitation study station in the northern AP, in addition to the moisture flux associated with the Mediterranean migratory depressions/cyclones, the local moisture flux enhancement via convection/topographic effects and/or linear cloud streaks from Sudan/Ethiopia may be the contributing factors for the precipitation during the wet season (see, for instance, Barth and Steinkohl 2004). In another case study, in the winter season, the local enhancement of the Mediterranean moisture flux was attributed mainly to the local topography (Chakraborty et al. 2006b). Based on the climatological and the thermodynamic analysis of several case studies in the AP, it was noticed that the local convection alone tend to fail because of the insufficient moisture flux supply in the AP (Babu et al. 2011).

Thus, an attempt is made to study the climatology and variability of the lower tropospheric moisture flux transport components over the AP, on a seasonal basis, in order to provide an updated context and perspective to the abovementioned studies. To this end, the relationships among the various moisture flux transport components are discussed over the AP on a seasonal basis, using a 53-year period climate dataset (1958–2010). Previously, the relationship between the moisture flux transport components and the precipitation occurrence over the AP has not been investigated, in detail, using such a long-term climatology (to our knowledge). An updated reference document on seasonal characteristics of the large-scale moisture flux transport over the AP is thus presented. Our study thus supplements and updates the earlier overlapping findings related to climatological behavior of the global large-scale moisture flux components (see, for instance, Dai 2006).

## 2 Data and methodology

The monthly gridded datasets for the $q$ and the zonal ($u$) and the meridional ($v$) wind components were obtained from the National Center for Environmental Protection-National Center for Atmospheric Research (NCEP–NCAR) reanalysis website (Kalnay et al. 1996; Kistler et al. 2001). The monthly gridded dataset for all the mandatory levels in the lower troposphere (1000, 925, and 850 hPa) is used for a 53-year period (1958–2010). The enhanced Climate Prediction Center (CPC) Merged Analysis of Precipitation (CMAP) monthly precipitation dataset was also obtained from the same website (Xie and Arkin 1997). The enhanced CMAP precipitation data starts from 1979. The enhanced CMAP dataset is used for a 32-year period (1979–2010). Both gridded datasets have a horizontal resolution of 2.5° latitude×2.5° longitude.

The NAO and AO monthly anomaly indices datasets, for 53 years, were obtained from the Climate Prediction Center (CPC) at the National Oceanic and Atmospheric Administration (NOAA) websites (http://www.cpc.ncep.noaa.gov/products/precip/CWlink/pna/nao.shtml, and http://www.cpc.ncep.noaa.gov/products/precip/CWlink/daily_ao_index/ao.shtml). The monthly NAO and AO anomaly indices are averaged to obtain the values for the two seasons used in this study.

The vertically integrated (large-scale) moisture flux transport in the air column may be represented by the integral of $q$ times the $u$ (and $v$) components of the wind over the pressure variable. The vertically integrated moisture flux vector $Q$ can be computed from the horizontal moisture flux as follows (Peixoto and Oort 1992):

$$\overline{Q} = \frac{1}{g} \int_{p_1}^{p_2} \overline{qV} dp, \tag{1}$$

where $V$ is the horizontal wind vector in meters per second, and $g$ is acceleration due to gravity in meters per squared second. In this study, the $Q$-vector describes the time-averaged seasonal picture of the moisture flux transport in units of kilograms per meter per second. The $p_1$ is the upper pressure level in the lower troposphere (850 hPa), and $p_2$ is the lower pressure level in the lower troposphere (1000 hPa). The over bar denotes a 53-year seasonal average.

The divergent component of the vertically integrated moisture flux vector $Q$ is calculated by taking the space derivatives of the field $\chi$ given by

$$\nabla^2 \chi = \nabla \cdot \overline{Q}. \tag{2}$$

The divergent component of the $Q$-vector indicates the sinks and sources of the large-scale moisture flux in units of kilograms per square meter per second. The field $\chi$ is calculated using the spectral methods found in Krishnamurti (1996).

The stream function field $\psi$ was obtained by solving the following equation for $\psi$ (see, for instance, Rosen et al. 1979):

$$\nabla^2 \psi = \widehat{k} \cdot \nabla \times \overline{Q}, \tag{3}$$

using the spectral methods. The seasonal net moisture flux, $F_W$, across each wall of the northern and southern domain in the AP is calculated using (Peixoto and Oort 1983; Chakraborty et al. 2006a)

$$F_W^{ew} = \frac{R}{g} \int_{p_1}^{p_2} \int_{\lambda_1}^{\lambda_2} \overline{qv} \cos\phi \, d\lambda dp, \tag{4}$$

for an east-west oriented wall, and

$$F_W^{ns} = \frac{R}{g} \int_{p_1}^{p_2} \int_{\phi_1}^{\phi_2} \overline{qu} \, d\phi dp, \tag{5}$$

for a north-south oriented wall. Here, $R$ denotes the radius of earth. The latitude is denoted by $\phi$, and the longitude is denoted by $\lambda$. The units of the net moisture flux are kilograms per second. The methods used here tend to capture the general large-scale features of the moisture flux transport over the AP.

The net moisture flux for the northern AP domain is given by

$$\Delta F_W^n = F_W^{AB} + F_W^{BC} + F_W^{CF} + F_W^{FA}, \qquad (6)$$

where moisture flux into (out of) the northern AP domain is taken as positive (negative). The east-west and north-south $F_W$ are given by Eqs. (4) and (5), respectively. A similar expression for the net moisture flux for the southern AP domain is used. Commonly used statistical methods are employed in this analysis (Wilks 2011). We are going to delve into the climatological behavior of these quantities next and will attempt to relate these with the AP seasonal precipitation patterns.

# 3 Results and discussion

## 3.1 The Somali Jet influence on the seasonal wind circulations over the AP

Figure 2 displays the seasonal horizontal wind vector distributions for the three mandatory levels in the lower troposphere over the study area. In the wet season, the wind circulation patterns are anticyclonic throughout the troposphere and increases with height. The progressively stronger northwesterly winds over the central AP in the upper levels of the lower troposphere tend to corroborate the dynamics of individual precipitation events in the winter season (Mujumdar 2006). In particular, at 850 hPa, the wind circulation from the Arabian Gulf to the Central/North AP regions is more pronounced. On the other hand, in the dry season, the horizontal wind vector distribution is of relatively lower magnitude reflecting the dominant presence of the Hadley cell-based high-pressure system and the intertropical convergence zone (ITCZ) over the AP (Walters and Sjoberg 1988). A lesser increase in the magnitude of winds occurs with height in the dry season, as compared to that in the wet season. Also noticeable is the direction reversal of the wind vectors at all levels in the lower troposphere in the south of the AP, over the Arabian Sea in the dry season as compared to the wet season. Furthermore, in the south of the AP, the wind vector magnitudes are large at lower levels (1000 and 925 hPa) with progressive southeastward shift in the magnitude and direction with height. These features are indicative of the onset and the eastward movement of the low level Somali Jet in the Arabian Sea (Findlater 1969).

## 3.2 The characteristics of the seasonal moisture flux transport components over the AP

Figure 3 displays the seasonal $q$ distribution for the three different isobaric levels in the lower troposphere. Even though the lower troposphere over AP is dominated by the high surface temperature occurrences (Almazroui et al. 2012a), a 53-year climatology of the $q$ distribution indicates that the lower tropospheric air remained relatively dry; typically of the order of 5–6 g kg$^{-1}$, during the two seasons, with the presence of a relatively weak meridional as well as a temperature gradient (not shown).

The $q$ distribution has relatively higher values in the dry season in the southern AP. This southern $q$ accumulation may be explainable in terms of the relatively lower temperatures. In the central AP, the temperatures are higher in lower tropospheric layers, whereas in the southwestern AP, relatively minimum temperatures occur (Almazroui et al. 2012b). Similar observations were noticed for the associated precipitable water content, in the lower troposphere, based on the $q$ behavior (not shown). The subsiding warm air is a contributing factor for this characteristic lower $q$ magnitude values between 15° N and 30° N over the AP (Walters and Sjoberg 1988). In the middle (925 hPa) and upper (850 hPa) troposphere, the $q$ value and the precipitable water content decreases, as compared to that in the lower troposphere (1000 hPa). As mentioned earlier, there is an indication of accumulation of higher $q$ over the Red Sea area in the southwestern AP. The relative accumulation of the $q$ over the extreme southwestern Red Sea and in the AP in the dry season is associated with the Sudan low/Red Sea trough (Abdelmola 2009). Comparing with the wind circulation patterns, unlike the vertical and spatial behavior of $q$, in the middle and upper troposphere, the wind circulation is more zonal (not shown).

The upper panels in Fig. 4 display the lower tropospheric transport of the moisture flux during the wet season for the 53-year period (1958–2010). The lower panels display the same for the dry season. The units for both panels are grams per kilogram per meter per second. In the wet season, over the Red Sea and the adjacent AP land areas, there is tongue of westward moisture flux transport, throughout the lower troposphere. The dominance of the 10 g kg$^{-1}$ m$^{-1}$ s$^{-1}$ isoline during the dry season over the AP is indicative of the mean location of the subsiding high-pressure system over the AP. At 1000 hPa, the eastward transport is noticeable in the dry season also, over and in the vicinity of the Red Sea. In the same season, over the Arabian Sea, the relatively large northeastward transport of the moisture flux is evident and consistent with the wind circulation patterns displayed in Fig. 2. The northward moisture flux transport is over the AP, whereas the southward transport of the moisture flux is over the Egypt and Sudan. In the dry season, as mentioned earlier, the dominance of the northeastward transport of the moisture
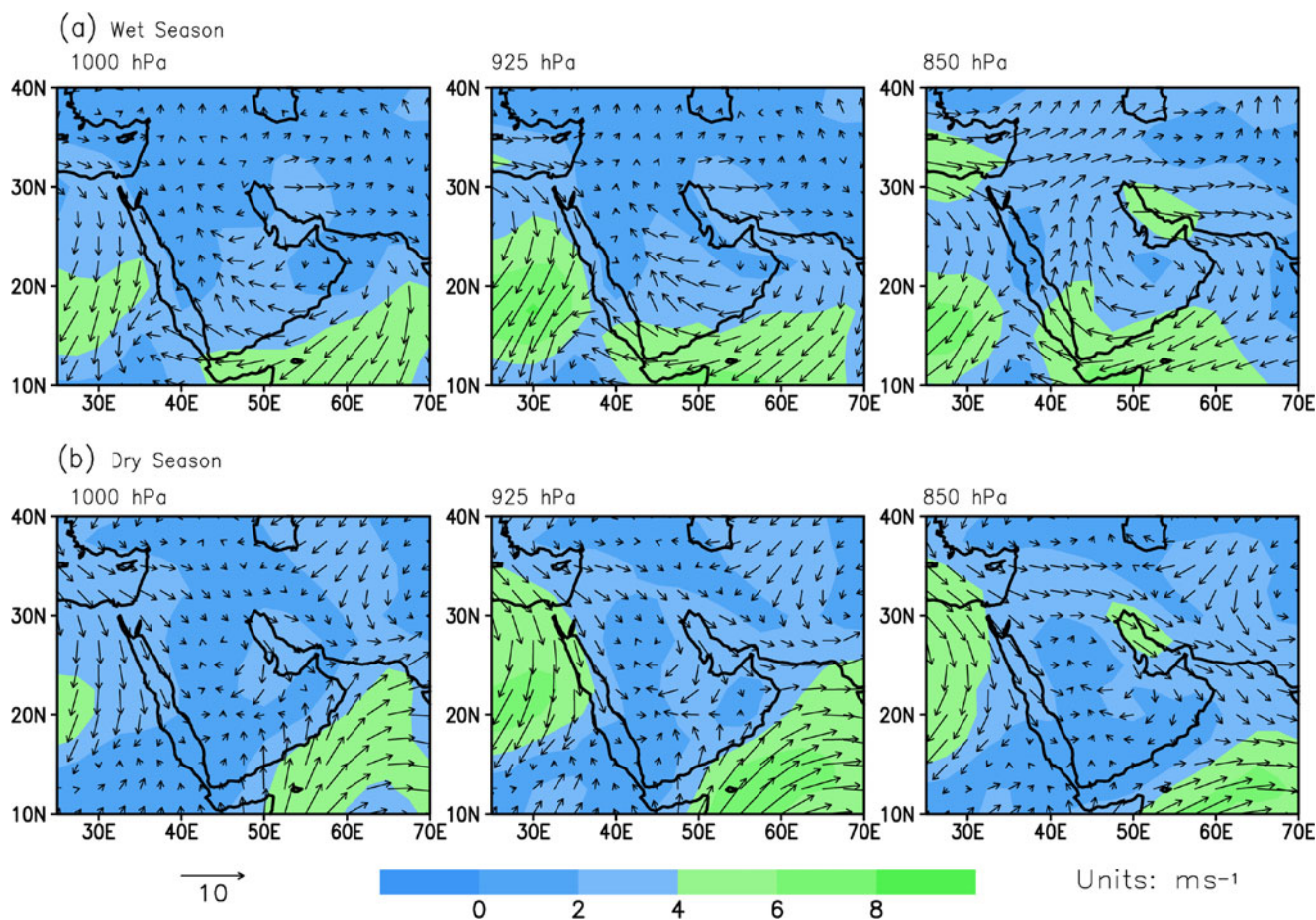
**Fig. 2** The horizontal distribution of the wind vectors (both magnitude and direction) at 1000, 925, and 850 hPa, for the **a** wet and the **b** dry season. Sample wind vector magnitude is displayed in the *lower left corner*

flux at the lower level in the Arabian Sea is noticeable. Thus, relatively less moisture flux is transported northward from the Arabian Sea into the AP land area in the dry season as compared to during the wet season. Analysis of separate zonal and meridional moisture flux transports on the monthly basis supports these findings (not shown).

In the wet season, in the lower troposphere, the magnitude of the meridional moisture flux transport is relatively higher, and it is progressively increasing with height. This higher level meridional transport of the moisture flux, though somewhat offset by the zonal moisture flux transport component, from the Arabian Sea may have contributed toward an individual precipitation event in the wet season (3 to 7 January 1996), as examined by Farajzadeh et al. (2007). Furthermore, during the wet season, the absence of the Somali Jet in the Arabian Sea allows some (net) moisture flux to penetrate into the southern and northern domains (see Fig. 1), whereas in the dry season, the moisture flux from the southern AP coast is strongly influenced by the Somali Jet, thus resulting in inflow of only very small (net) moisture flux into the AP land area. In the dry season, there is also a dominance of the Hadley cell-based high-pressure system, resulting in relatively even lower

precipitation. This is consistent with the enhanced CMAP precipitation climatology displayed in Fig. 7b.

**3.3 The moisture flux transport and the precipitation over the AP**

Figure 5 displays the absolute magnitude and direction of the vertically integrated $Q$-vector over the AP on the seasonal basis, within the lower troposphere, using Eq. (1). The dominating northward intrusion of the Arabian Gulf moisture into the southern and central AP areas contributes toward the precipitation in the wet season by corroborating with the relatively lower temperatures available in the central and northern AP. This large-scale northward anti-cyclonic intrusion of the moisture flux into the AP during the wet season may act as an enhancement factor for the transient disturbances giving rise to the individual precipitation events depending upon the spatial and the temporal details of the selected case study event (Mujumdar 2006). Though there is small contribution of the moisture flux from the Mediterranean Sea in the dry season, however because of the high-pressure sustenance/warmer temperatures over the AP during this season, this moisture
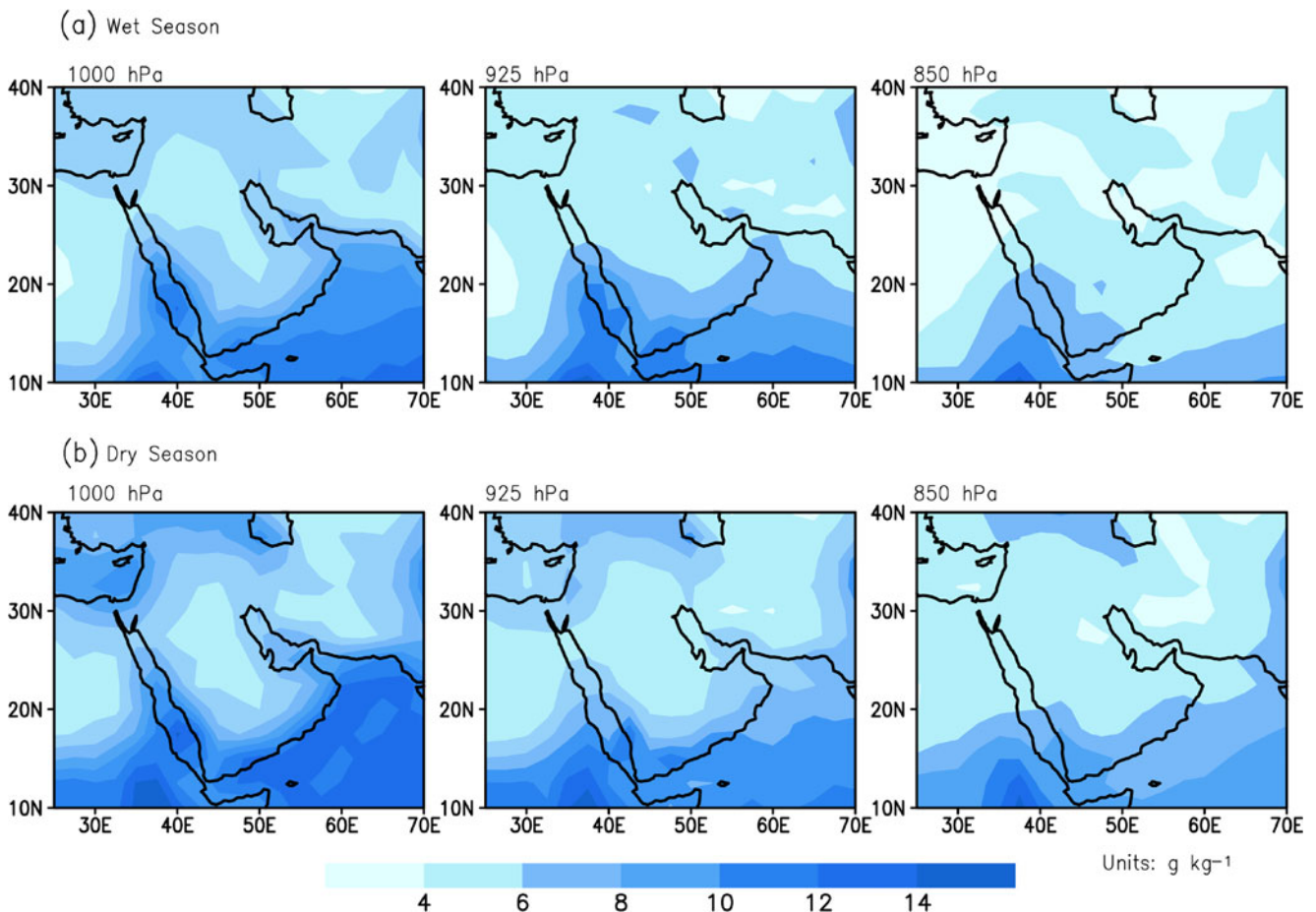
**Fig. 3** The specific humidity, $q$ (g kg$^{-1}$) at 1000, 925, and 850 hPa, for the **a** wet and **b** dry season. The shading interval is 2 g kg$^{-1}$ for both seasons

flux does not seem to play a dominant role in the precipitation over the AP. During both the seasons, there is moisture supply from the Mediterranean Sea into the Red Sea (relatively higher in the dry season). This moisture flux is transported into the east Africa reaching the Ethiopian plateau through Eritrea mountain chain, during the dry season (Viste and Sorteberg 2013a; Viste and Sorteberg 2013b). The seasonal horizontal distribution of the Q-vector displayed in Fig. 5 is similar to the findings by Zhu and Newell (1998).

Figure 6 displays the divergent component of the vertically integrated Q-vector, on the seasonal basis, using Eq. (2). In the dry season, between approximately 15° N and 20° N, the northward migration of the ITCZ contributes toward the convergence of the moisture flux in the lower troposphere over the eastern Sudan and the southwest of the AP. The patterns of the divergent components of the moisture flux over the AP bear some resemblance with the seasonal precipitation patterns displayed in Fig. 7. There is small precipitation in the southwest region of the AP in the dry season, associated with the northward movement of the ITCZ over the AP. This is also consistent with the dry season precipitation patterns over the southern Yemen and southern Oman (Charabi 2009). The

main source of the moisture flux during the dry season is the Arabian Sea.

In the wet season, there is convergence of the moisture flux over the south and the central AP. Comparing it with Fig. 7a, which displays the precipitation (albeit very small) during the wet season, we note a general consistency between the two. Namely, the large-scale moisture flux convergence contributes toward precipitation in the wet season over the AP. During the wet season, the AP receives the moisture flux from the Red Sea, Arabian Sea, and to some extent from the Mediterranean Sea. These patterns of the moisture flux convergence and divergence are consistent with the convergence and divergence patterns found in a 43-year period moisture flux climatology by Chakraborty et al. (2006b). This is indicative of the existence of climatological robustness of the large-scale moisture flux patterns.

The seasonal CMAP climatology for the AP and the adjacent areas is displayed in Fig. 7. As has been indicated in several of the recent studies, the precipitation occurrence is dominated during the wet season in the AP (Almazroui et al. 2012b, and references cited therein). During the dry season, the precipitation is confined to the southwestern region of the AP. This is in agreement with the features of divergence of the
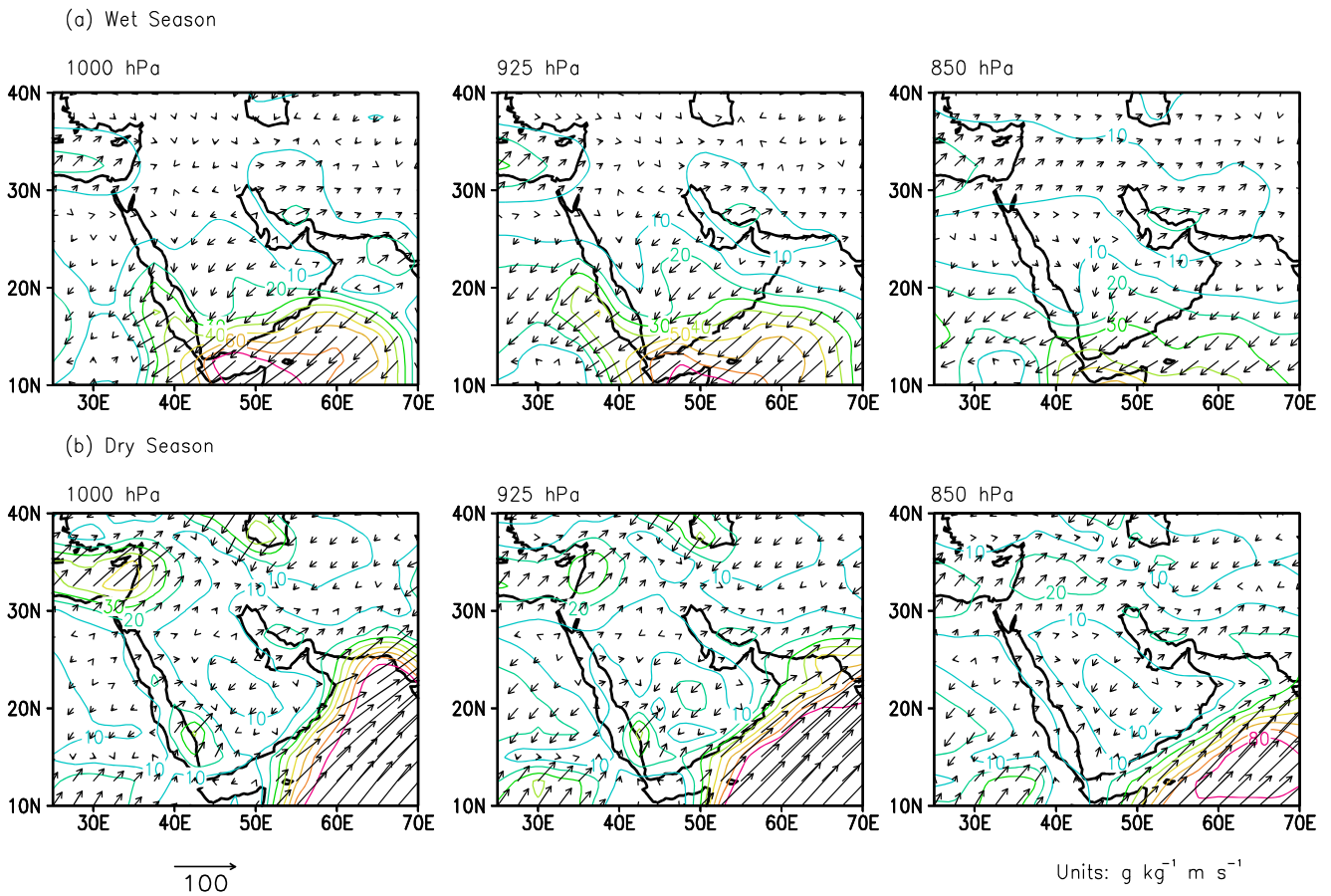
(a) Wet Season

1000 hPa    925 hPa    850 hPa

(b) Dry Season

1000 hPa    925 hPa    850 hPa

100

Units: g kg$^{-1}$ m s$^{-1}$

**Fig. 4** The transport of the moisture flux at 1000, 925, and 850 hPa, for the **a** wet and the **b** dry season. The contour interval is 10 g kg$^{-1}$ ms$^{-1}$ for both seasons. The sample moisture flux vector magnitude is displayed in the *lower left corner*
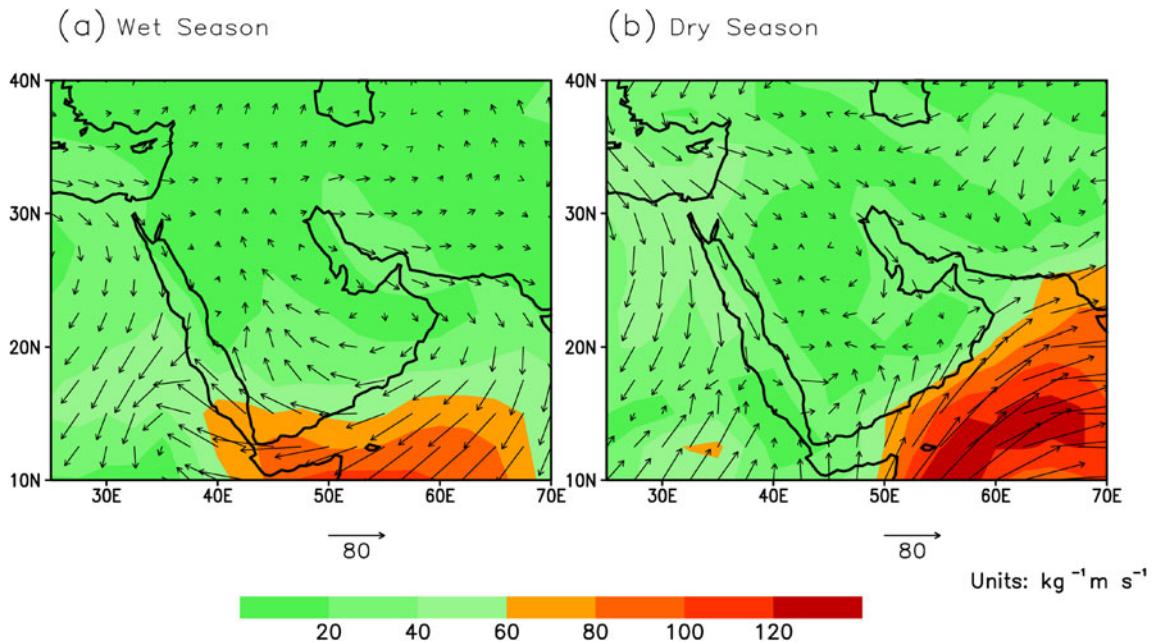
(a) Wet Season    (b) Dry Season

80    80

Units: kg$^{-1}$ m s$^{-1}$

20    40    60    80    100    120

**Fig. 5** The vertically integrated *Q*-vector (magnitude and direction) for the lower troposphere, for the **a** wet and the **b** dry season. The sample *Q*-vector magnitude is displayed at the bottom of each panel
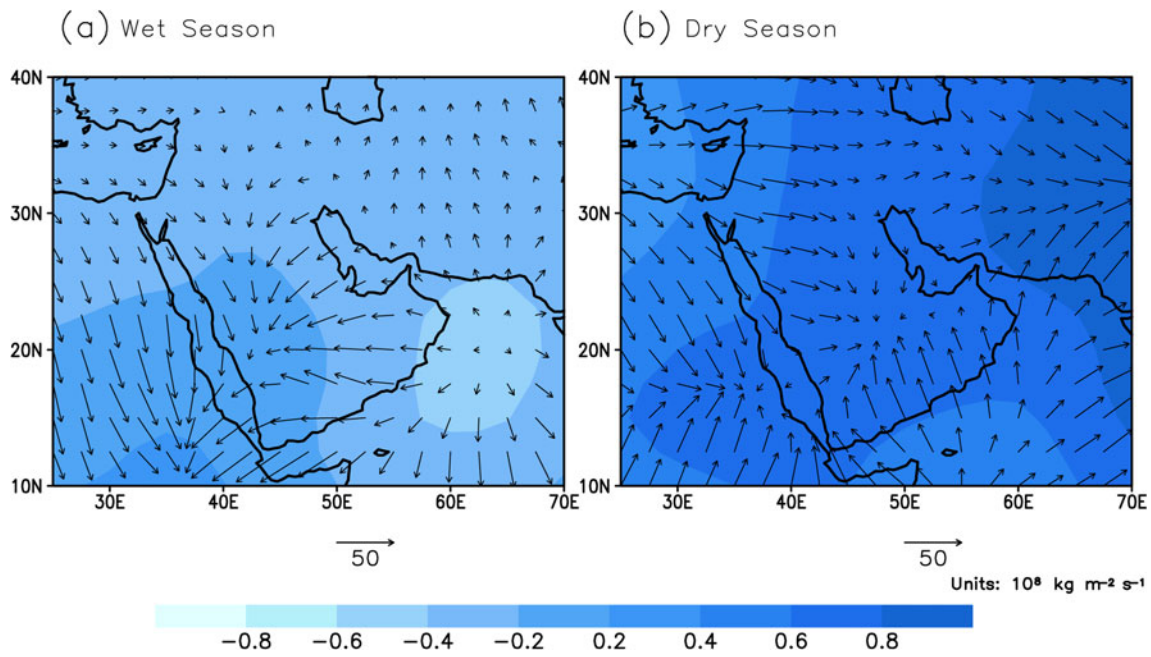
**Fig. 6** The divergent component of the vertically integrated $Q$-vector for the lower troposphere, for the **a** wet and the **b** dry season in units of $10^8$ kg m$^{-2}$ s$^{-1}$. The sample vector magnitude is displayed at the *bottom of each panel*

$Q$-vector displayed in Fig. 6, as discussed earlier. The techniques used in this paper to diagnose the possible relationship between the large-scale moisture flux transport and the precipitation over the AP are thus capturing and identifying resemblance in the two quantities, to some extent. The relative higher precipitation in the wet season in the northeast AP (in the northern AP domain) is consistent with the annual cycle of the precipitation in the Kuwait City (Marcella and Eltahir 2008).

The investigation of the cause of relatively small seasonal precipitation over the AP is beyond the scope of this study. It is sufficient to state that mechanisms are being suggested to provide reasons for the negligibly small precipitation over the AP including the increased albedo feedback effect resulting in the possible enhancement in the Hadley cell related decent (Charney 1975), and the possible relationship between the remote diabatic heating in the Asian monsoon region and the
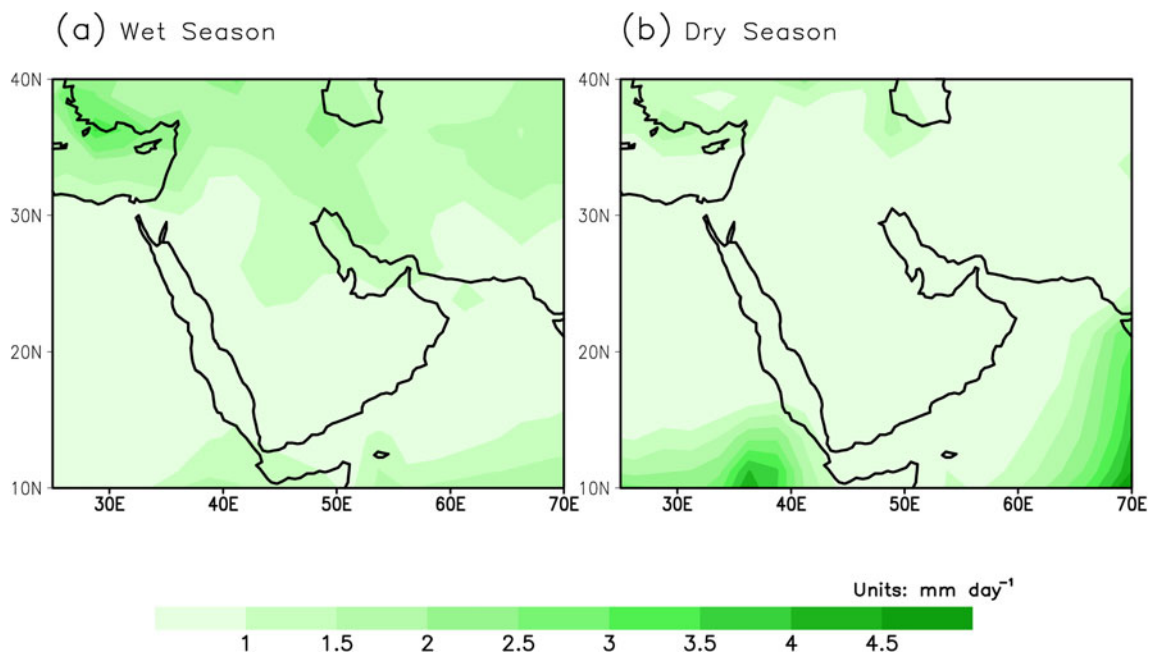


**Fig. 7** The enhanced CMAP precipitation climatology for the **a** wet and the **b** dry season. The shading interval is 0.5 mm day$^{-1}$

precipitation dynamics of the Arabian Desert via the Rossby wave propagation (Rodwell and Hoskins 1996).

### 3.4 The stream function field analysis

Figure 8 displays the seasonal stream function field distribution over the AP including the adjacent area, using Eq. (3), in units of kilograms per second. The stream function field reveals more moisture circulation structure than obtainable from the low level wind field or the zonal and meridional moisture flux transport vectors alone (see, for instance, Rosen et al. 1979).

The vertically integrated stream function field over the AP indicates that, in the wet season, an anticyclonic Peninsula-size circulation from the Arabia Sea into the AP exists. This circulation contributes toward the wet season moisture flux for the AP region, in the absence of the low level Somali Jet. In the dry season, moisture flow from the Mediterranean is limited to the extreme North of the AP (~30° N). In this season, the anticyclonic moisture flux flow is present over Egypt and Sudan. Also, in this season, presence of the relatively lower magnitude of Arabian Sea moisture flux is noticeable in the south of the AP because of the Somali Jet. In the dry season, the patterns of the Q-vector and the stream function field are more similar.

### 3.5 The moisture budget analysis

Figure 9 displays the vertically integrated mean climatological moisture flux values across all the walls of the two domains displayed in Fig. 1, using Eqs. (4), (5), and (6), in units of $10^6$ kg s$^{-1}$. For each wall, the direction of the arrow indicates

the climatological net moisture flux transport direction through that wall. The number in the circle in each domain for each season quantifies the algebraic sum of the net moisture flux through each wall of the domain.

In the dry season, the dominant source of the moisture flux into the southern AP is the Arabian Sea/tropical belt; in particular through the wall ED, it amounts to $190 \times 10^6$ kg s$^{-1}$. The net moisture flux through this wall is sensitive with respect to its location. During the dry season, the magnitude of the net moisture flux is relatively larger as compared to the wet season, in the southern AP domain. The eastward transfer of $170 \times 10^6$ kg s$^{-1}$ of the moisture flux from the wall CD is associated with the presence of Somali Jet in the dry season.

In the wet season, the net moisture flux transport is relatively small as compared to the net moisture flux transport during the dry season, in the particular in the southern AP domain. There is net moisture flux transport out of the northern most wall AB in the northern domain in the wet season. Also, there is net moisture flux transport from the northern AP domain in the wet season from the wall BC. This behavior is consistent with the discussion in Sect. 3.2 about the moisture flux transport into the western Iran over the AP in the wet season. The net moisture flux gain in the northern domain (displayed in the circle) in the winter season is indicative of the widespread precipitation in the northern AP domain (≥22° N).

### 3.6 The teleconnections with the NAO and the AO climatic indices

It was noticed that a sea level pressure teleconnection pattern between the AP and North Pacific Ocean (NPO) may exist
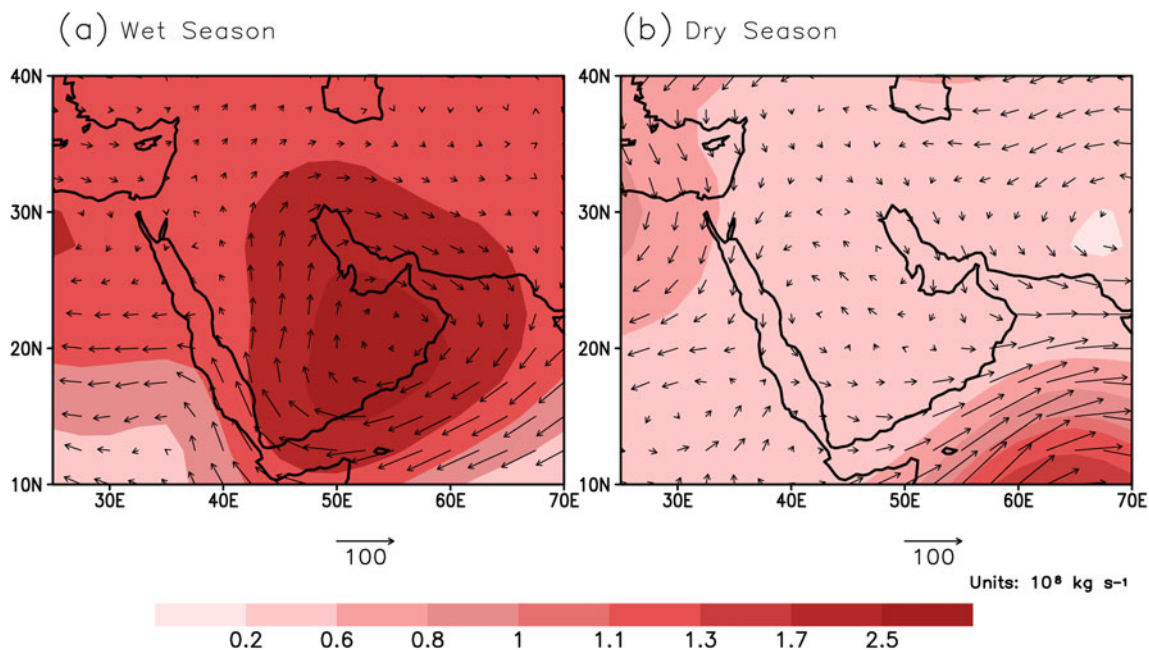


**Fig. 8** The seasonal stream function field climatology for the lower troposphere, for the **a** wet and the **b** dry season. The sample magnitude of the stream function field is displayed at the bottom of each panel

**Fig. 9** The vertically integrated lower tropospheric net moisture flux through each wall of the southern and northern AP domain displayed in Fig. 1, for the **a** wet and the **b** dry season in units of $10^6$ kg s$^{-1}$



(a) Wet Season
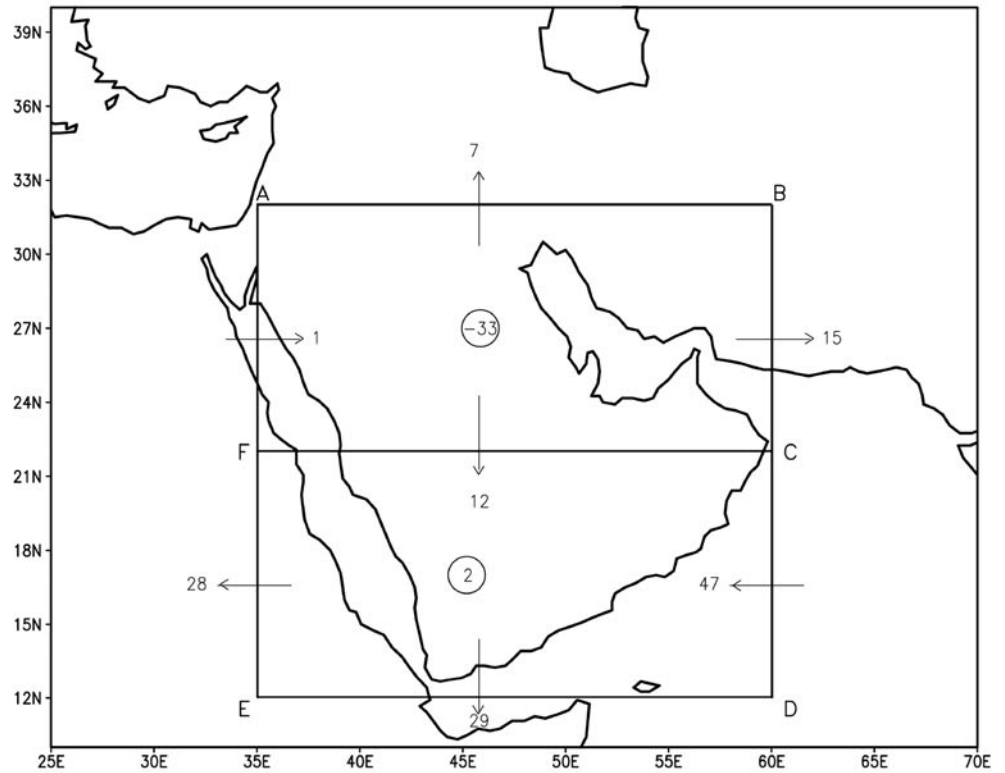


(b) Dry Season
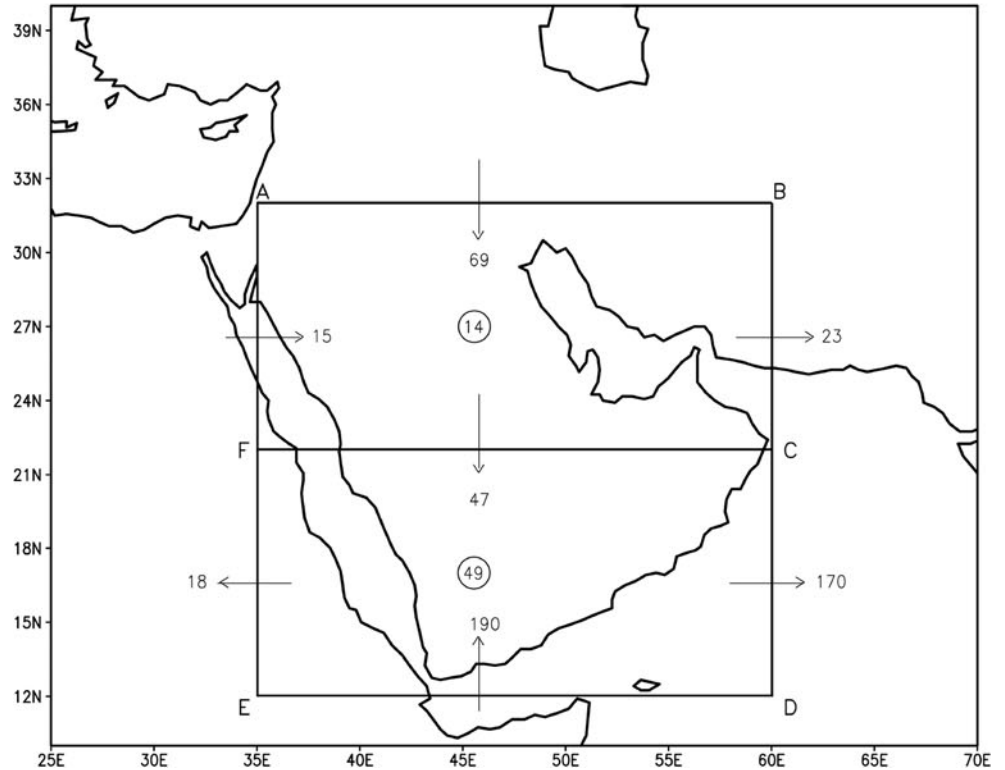
(JianQi et al. 2008). In the same study, a covariation between the two was noticed in the dry season based on a 57-year NCEP-NCAR reanalysis gridded dataset. Associated moisture flux transport over south Asia and north China was also discussed by JianQi et al. (2008). In a separate study, the relationship of the Indian Ocean Dipole (IOD) and the El-Niño Southern Oscillations (ENSO) climatic indices with the net moisture flux over Saudi Arabia in the AP was discussed by Chakraborty et al. (2006a). It was pointed out that through the Red Sea, the net moisture flux is enhanced in the simultaneous presence of the positive IOD and the warm phase of the ENSO.

These studies are suggestive of the observation that the large-scale climatic indices do play a role in determining the seasonal variability of the net moisture flux transport over the AP. This motivated us to investigate this aspect further. Here, we report the results for the NAO and AO teleconnection correlation coefficients (CC) with the net moisture flux transport over the AP. To our knowledge, this aspect has not been discussed earlier. It has been noticed earlier that the large-scale atmospheric moisture budget over the northern Europe is affected differently in various phases of the NAO via a shift in the storm tracks (Hurrell 1995), as well as over the Arctic Ocean (Dickson et al. 2000). For a recent review of various aspects of the NAO climatic index, see Pinto and Raible (2012).

The CCs between the time series of the net moisture flux through each wall and the NAO and the AO climatic indices were calculated on the seasonal basis for both the domains in the AP. The results are displayed in Table 1. According to Table 1, both indices contribute toward the net seasonal moisture flux modulation over the AP, in a statistically significant manner, with confidence level (CL) >95 %. Let us note that an out-of-phase CC is obtained between the NAO and the AO climatic indices and the net moisture flux over the AP in this study. An in-phase CC was found between the IOD and the

ENSO climatic indices, using different domains inside the AP land area, by Chakraborty et al. (2006a).
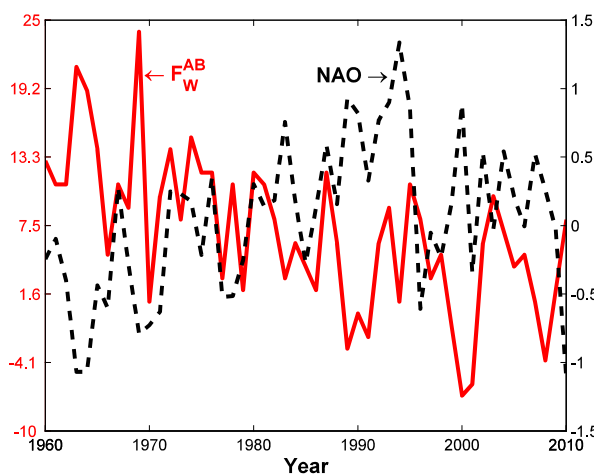
Figure 10 displays an example of the out-of-phase interannual covariability of the net moisture flux through the wall AB in the northern AP domain in the wet season with the NAO and AO climatic indices. No smoothing filter is applied in order to display the absolute magnitude of values. The maximal NAO-positive phase occurs during the wet season for the year 1994, with anomaly index value of 1.34, corresponding to a relatively lower value for $F$ as approximately $1 \times 10^6$ kg s$^{-1}$. The climatological mean value for $F$ was $7 \times 10^6$ kg s$^{-1}$, whereas the standard deviation was $6.4 \times 10^6$ kg s$^{-1}$. The relatively large standard deviation is indicative of relatively large interannual variability in the net moisture flux. This and other statistically significant teleconnection correlations may have some relevance for the seasonal predictions of the net moisture flux transport over the AP. A linear

**(a) NAO and net moisture flux co-variability in northern AP**



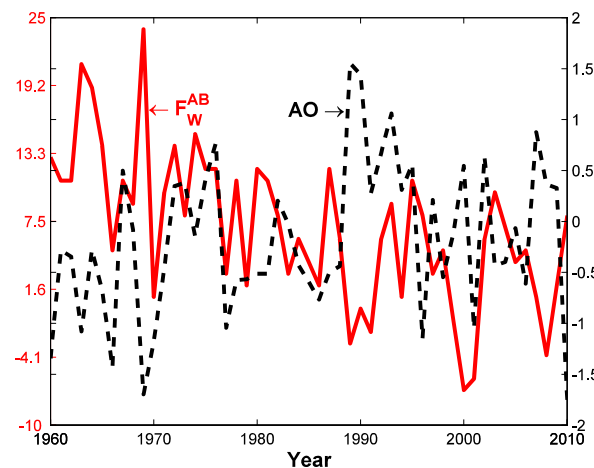**(b) AO and net moisture flux co-variability in northern AP**



**Fig. 10** The interannual variability of the vertically integrated net moisture flux through the wall AB (in units of $10^6$ kg s$^{-1}$) during the wet season, and the **a** NAO and **b** AO climatic index for the period of study

**Table 1** The seasonal CC of the vertically integrated net moisture flux through the walls of the two domains with the NAO and AO climatic indices for the 53-year period

| Domain | Season-domain | NAO | AO |
|---|---|---|---|
| Northern | Wet-AB | −0.41 | −0.30 |
| | Dry-FC | −0.34 | −0.34 |
| Southern | Wet-ED | −0.28 | −0.31 |
| | Wet-CD | −0.43 | −0.45 |
| | Dry-FC | −0.34 | −0.34 |
| | Dry-CD | | 0.28 |

The second column displays the boundary wall across which the CC between the NAO and the AO and the vertically integrated net moisture flux is calculated. The next two columns under the NAO and AO display the CC values with the confidence level (CL) greater than 95 %, respectively

trend analysis for the seasonal net moisture flux through both AP domains was also performed. In general, a decreasing linear trend of the net seasonal moisture flux through all the walls is noticed, with statistically more robust linearly decreasing trend during the wet season, as compared to that in the dry season (not shown).

The wet season positive and negative NAO and AO phases have distinct related moisture flux covariability through the northern wall AB. The positive and negative phases of NAO and AO were obtained following López-Moreno and Vicente-Serrano (2008). This amounts in separating values of seasonal NAO and AO indices having value greater (less) than +0.45 (−0.45). This procedure entailed the following 12 (10) positive NAO (AO) phase years during the 53-year period study: 1983, 1987, 1989, 1990, 1992, 1993, 1994, 1995, 2000, 2002, 2004, and 2007 (1967, 1976, 1989, 1990, 1992, 1993, 1995, 2000, 2002, 2007). The following 10 (20) negative phase NAO (AO) years were also obtained: 1963, 1964, 1966, 1969, 1970, 1971, 1977, 1978, 1996, and 2010 (1960, 1963, 1965, 1966, 1969, 1970, 1971, 1977, 1978, 1979, 1980, 1981, 1985, 1986, 1987, 1996, 1998, 2001, 2006, 2010). The remaining years were counted as neutral. The NAO and AO leads to shift in wind pattern that modulates the moisture flux over Europe and Mediterranean region (see, for instance, Ambaum et al. 2001). In particular, when NAO is in negative phase, more moisture flux transport occurs through the wall AB, and vice versa. Since, for instance, with negative NAO phase, the southward shift of the storm tracks brings more moisture flux into the southern Mediterranean Sea area (see, for instance, Hurrell et al. 2003). In the wet season, which includes the conventional winter or DJF season, the NAO and AO modulate the storm tracks more strongly over and in AP, thus resulting in more moisture flux supply into northern AP.

## 4 Conclusions

Over the AP, the seasonal characteristics of the lower tropospheric (1000 to 850 hPa) large-scale moisture flux transport including the moisture budget are studied using the NCEP-NCAR monthly gridded dataset for a 53-year period (1958–2010). In the dry season (June to September), in the southern AP domain (≤22° N), the time-mean moisture flow is dominated by the Arabian Sea moisture flux intake. It is noted that the AP serves as a moisture flux transporter to the adjacent countries such as western Iran.

Relatively lower specific humidity values dominate the AP land area during both the wet (November to April) and dry seasons, typically of the order of 5–6 g kg$^{-1}$, in the lower troposphere. This is related to the persistent dominance of the Hadley cell-based descent over the AP. In the dry season, in the southwestern part of the AP, the lower tropospheric

specific humidity values are higher in the dry season, owing to the existence of the Sudan low and its extended tongue in the form of Red Sea trough.

As a related aspect, the existence of zero isoline for both the total zonal and the meridional moisture flux transport components during both the seasons is indicative of dominance of Hadley cell-based subsidence over the AP thus contributing toward the formation of the spatial and the temporal precipitation patterns.

The horizontal distribution of the vertically integrated seasonal divergent field patterns of the $Q$-vector and the precipitation patterns over the AP seems to have some resemblance. This may be indicative of the role played by the large-scale moisture flux transport in the seasonal precipitation over the AP. The convergence field of the $Q$-vector over the AP land area in the wet season may explain the wide spread precipitation in the wet season. The east-west oriented convergence field of the $Q$-vector localized in the southern AP may explain the localized dry season precipitation.

The vertically integrated seasonal $Q$-vector and the stream function field analysis reveal the structure of the large-scale moisture flux circulations over the AP including the adjacent areas. In the wet season, moisture flux inflow from the Arabian Gulf and the Arabian Sea seems to supply the requisite moisture flux (in the absence of the low level Somali Jet) that may get local enhancement under favorable conditions, to cause individual precipitation events in the northern AP. In the dry season, considerable southeastward moisture flux transport occurs in the vicinity of the southern AP boundary, mainly due to the presence and eastward movement of the Somali Jet; however, the cumulative inflow of the moisture flux into the AP is small in this season.

Our obtained results are in general agreement with those obtained by Chakraborty et al. (2006a) concerning the moisture flux transport over Saudi Arabia, vis-à-vis: (i) large-scale moisture flux alone is not the only contributing factor toward precipitation occurrence over Saudi Arabia and that (ii) the large-scale climatic indices have impact on the net moisture flux transport over the AP. An out-of-phase and statistically significant (CL>95 %) seasonal teleconnection correlation was found between both the NAO and the AO climatic indices and the net moisture flux in the lower troposphere, over the AP.

## References

Abdelmola YK (2009) Surface synoptic type over central Sudan during 1994–2003. Ph.D. Dissertation. Aristotle University

Almazroui M, Islam MN, Athar H, Jones PD, Rahman MA (2012a) Recent climate change in the Arabian Peninsula: annual rainfall and temperature analysis of Saudi Arabia for 1978–2009. Int J Climatol 32:953–966. doi:10.1002/joc.3446

Almazroui M, Islam MN, Jones PD, Athar H, Rahman MA (2012b) Recent climate change in the Arabian Peninsula: seasonal rainfall and temperature climatology of Saudi Arabia for 1979–2009. Atmos Res 111:29–45. doi:10.1016/j.atmosres.2012.02.013

Almazroui M, Abid MA, Athar H, Islam MN, Ehsan MA (2013) Interannual variability of rainfall over the Arabian Peninsula using the IPCC AR4 Global Climate Models. Int J Climatol 33:2328–2340. doi:10.1002/joc.3600

Ambaum HPM, Hoskins BJ, Stephenson DB (2001) Arctic Oscillation or North Atlantic Oscillation? J Clim 14:3495–3507

Athar H, Almazroui M, Islam MN, Abid MA, Ehsan MA (2013) Effect of mid-latitude blocking anticyclones on the weather of the Arabian Peninsula. Int J Climatol 33:585–598. doi:10.1002/joc.3450

Athar H (2014) Trends in observed extreme climate indices in Saudi Arabia during 1979–2008. Int J Climatol 34:1561–1574. doi:10.1002/joc.3783

Athar H (2015) Teleconnections and variability in observed rainfall over Saudi Arabia during 1978–2010. Atmos Sci Lett. doi:10.1002/asl2.570

Babu CA, Samah AA, Varikoden H (2011) Rainfall climatology over Middle East region and its variability. Int J Water Resour Arid Environ 1(3):180–192

Barth H-J, Steinkohl F (2004) Origin of winter precipitation in the central coastal lowlands of Saudi Arabia. J Arid Environ 57(1):101–115

Chakraborty A, Behera SK, Mujumdar M, Ohba R, Yamagata T (2006a) Diagnosis of tropospheric moisture over Saudi Arabia and influences of IOD and ENSO. Mon Weather Rev 134:598–617

Chakraborty A, Mujumdar M, Behera SK, Ohba R, Yamagata T (2006b) A cyclone over Saudi Arabia on 5 January 2002: a case study. Meteorol Atmos Phys 93:115–122

Charabi Y (2009) Arabian summer monsoon variability: teleconexion to ENSO and IOD. Atmos Res 91:105–117

Charney JG (1975) Dynamics of deserts and drought in the Sahel. Q J R Meteorol Soc 101(428):193–202. doi:10.1002/qj.49710142802

Dai A (2006) Recent climatology, variability, and trends in global surface humidity. J Clim 19:3589–3606. doi:10.1175/JCLI3816.1

Dickson RR, Osborn TJ, Hurrell JW, Meincke J, Blindheim J, Adlandsvik B, Vinje T, Alekseev G, Maslowski W (2000) The Arctic Ocean response to the North Atlantic oscillation. J Clim 13:2671–2696

Edgell HS (2006) Arabian deserts: nature, origin and evolution. Springer, The Netherlands

Farajzadeh M, Ahmadabad MK, Ghaemi H, Mobasheri MR (2007) Studying the moisture flux over west of Iran: a case study of January 1 to 7, 1996 rain storm. J Appl Sci 7(20):3023–3030

Findlater J (1969) A major low-level air current near the Indian Ocean during the northern summer. Q J Roy Meteorol Soc 95:362–380

Gimeno L, Nieto R, Drumond A, Durán-Quesada AM, Stohl A, Sodemann H, Trigo RM (2011) A close look at oceanic sources of continental precipitation. Eos 92(23):193–194

Halpern D, Woiceshyn PM (1999) Onset of the Somali Jet in the Arabian Sea during June 1997. J Geophys Res 104(C8):18041–18046. doi:10.1029/1999JC900141

Hurrell J (1995) Decadal trends in the North Atlantic oscillation: regional temperatures and precipitation. Science 269(5224):676–679. doi:10.1126/science.269.5224.676

Hurrell JW, Kushnir Y, Ottersen G, Visbeck M (2003) An overview of the North Atlantic Oscillation. In: Hurrell JW, Kushnir Y, Ottersen G, Visbeck M (eds) The North Atlantic Oscillation: climate significance and environmental impact, Geophys Monogr 134. Am Geophys Union, Washington, USA, pp 1–36

IPCC (2013) Climate Change. The Physical Science Basis. Contribution of Working Group I to the Fifth Assessment Report of the Intergovernmental Panel on Climate Change, Stocker TF, Qin D, Plattner G-K, Tignor M, Allen SK, Boschung J, Nauels A, Xia Y, BexV and Midgley PM (eds). Cambridge University Press, Cambridge, 1535 p.

JianQi S, Wei Y, YuZhong G (2008) Arabian Peninsula-North Pacific Oscillation and its association with the Asian summer monsoon. Sci China Ser D Earth Sci 51(7):1001–1012

Jin F, Kitoh A, Alpert P (2011) Climatological relationships among the moisture budget components and rainfall amounts over the Mediterranean based on a super-high-resolution climate model. J Geophys Res 116, D09102

Kalnay E, Kanamitsu M, Kistler R, Collins W, Deaven D, Gandin L, Iredell M, Saha S, White G, Woollen J, Zhu Y, Chelliah M, Ebisuzaki W, Higgins W, Janowiak J, Mo KC, Ropelewski C, Wang J, Leetmaa A, Reynolds R, Jenne R, Joseph D (1996) The NCEP/NCAR 40-year reanalysis project. Bull Am Meteorol Soc 77:437–471

Kistler R, Kalnay E, Collins W, Saha S, White G, Woollen J, Chelliah M, Ebisuzaki W, Kanamitsu M, Kousky V, Hvd D, Jenne R, Fiorino M (2001) The NCEP-NCAR 50-year reanalysis: monthly means CD-ROM and documentation. Bull Am Meteorol Soc 82:247–267

Krishnamurti T N (1996) An introduction to numerical weather prediction techniques. CRC Press

López-Moreno JI, Vicente-Serrano SM (2008) Positive and negative phases of the wintertime North Atlantic Oscillation and drought occurrence over Europe: a multitemporal-scale Approach. J Clim 21:1220–1243

Marcella MP, Eltahir E (2008) The hydroclimatology of Kuwait: explaining the variability of rainfall at seasonal and interannual time scales. J Hydrometeorol 9:1095–1105. doi:10.1175/2008JHM952.1

Min W, Schubert S (1997) The climate signal in regional moisture fluxes: a comparison of three global data assimilation products. J Clim 10:2623–2642

Mujumdar M (2006) Diagnostic analysis of wintertime rainfall events over the Arabian region. ISSN 0252−1075, Indian Institute of Tropical Meteorology Research Report No. RR−111

Peixoto JP, Oort AH (1983) The atmospheric branch of the hydrological cycle and climate. Variations of the global water budget, Reidel, pp 5–65

Peixoto JP, Oort AH (1992) Physics of climate. AIP Press

Pinto JG, Raible CC (2012) Past and recent changes in the North Atlantic Oscillation. WIREs Clim Chang 3:79–90. doi:10.1002/wcc.150

Prasanna V, Yasunari T (2011) Simulated changes in the atmospheric water balance over South Asia in the eight IPCC AR4 coupled climate models. Theor Appl Climatol 104:139–158. doi:10.1007/s00704−010−0331−6

Rodwell MR, Hoskins BJ (1996) Monsoons and the dynamics of deserts. Q J Roy Meteorol Soc 122:1385–1404

Rosen RD, Salstein DA, Peixoto JP (1979) Streamfunction analysis of interannual variability in large-scale water vapor flux. Mon Weather Rev 107:1682–1684

Sherwood SC, Roca R, Weckwerth TM, Andronova NG (2010) Tropospheric water vapor, convection, and climate. Rev Geophys 48, RG2001. doi:10.1029/2009RG000301

Starr VP, Peixoto JP (1958) On the global balance of water vapour and the hydrology of deserts. Tellus 10(2):188–194

Trenberth KE (2011) Change in precipitation with climate change. Clim Res 47:123–138

Vincent P (2008) Saudi Arabia: an environmental overview. Taylor and Francis, London

Viste E, Sorteberg A (2013a) Moisture transport into the Ethiopian highlands. Int J Climatol 33:249–263. doi:10.1002/joc.3409

Viste E, Sorteberg A (2013b) The effect of moisture transport variability on Ethiopian summer precipitation. Int J Climatol 33:3106–3123. doi:10.1002/joc.3566

Walters KR Sr, Sjoberg WF (1988) The Persian Gulf region: a climatological study. USAF Environmental Technical Applications Center, Scott Air Force Base, Illinois, 62225–5438, USA. Technical report No. USAFETAC/TN–88/002 (AD–A222 654)

Wilks DS (2011) Statistical methods in the atmospheric sciences, 3rd edn. Elsevier publishers, New York, USA

Xie P, Arkin PA (1997) Global precipitation: a 17-year monthly analysis based on gauge observations, satellite estimates, and numerical model outputs. Bull Am Meteorol Soc 78:2539–2558

Zhu Y, Newell RE (1998) A proposed algorithm for moisture fluxes from atmospheric rivers. Mon Weather Rev 126:725–735